Tunneling spectroscopy by matching energy levels in the spin-rotating frame

Changho Choi and M. M. Pintar
Department of Physics, University of Waterloo, Waterloo, Ontario, Canada N2L 3G1
(Received 30 September 1996)

Tunneling spectra of strongly hindered CH_3 in methylmalonic acid, dimethyl sulfide, propionic acid, and hexane are reported. The Zeeman-tunneling level-matching resonances are detected at $\omega_Z = n\omega_T$, $n = \frac{1}{4}$, $\frac{1}{3}$, $\frac{1}{2}$, $\frac{2}{3}$, 1, and 2 when the level matching is maintained for 10 ms in the 54.7° tilted proton spin-rotating frame. A ground-state manifold of two noninteracting but equivalent methyl groups accounts for these spectra. All the transitions, which bring about the population equalization whenever a matching resonance occurs, are driven by time-independent dipole-dipole interactions. The resonance peaks at $\omega_Z = \frac{2}{3}\omega_T$ and $\omega_Z = 2\omega_T$, which are observed in a tilted rotating frame only, indicate that pairs of methyl groups undergo a symmetry conversion simultaneously. The calculated magnetization changes, which are the consequence of population equilibration, reproduce the observed resonance peaks intensities well. [S0163-1829(97)04934-5]

I. INTRODUCTION

It has been shown recently[1] that level-matching NMR in the spin-rotating frame is a good technique for tunneling studies of strongly hindered CH_3 groups at low temperatures. The transfer of polarization occurs as a result of matching a precooled nuclear Zeeman state to a tunneling state at lattice temperature. After this step the rotating frame is removed, only to reintroduce the same level matching a few ms later with all Zeeman states equally populated. In the second-level matching pulse the tunneling states are still strongly polarized and are used to polarize the saturated nuclear spins. Following this tunneling to Zeeman polarization transfer a considerable nuclear spin magnetization is detected. The magnetization monitored as a function of Zeeman splitting gives the level-matching tunneling spectrum. Establishment of a level-matching resonance for a long time enables even the weak second-order transitions to bring about a measurable polarization transfer.

The dipolar Hamiltonian which drives the transitions between matched levels can be manipulated experimentally by tilting the effective field in the rotating frame.[1–3] If the effective field is tilted from 90° to 45° with respect to the main magnetic field H_0 the form of the dipolar interaction changes considerably. In this way the particular quantum number change Δm can be established for all transitions. The even quantum-number transitions ($|\Delta m| = 2,4,\ldots$) are driven in the normal rotating frame with $\theta = 90°$. If the effective field is less tilted, the odd quantum-number transitions ($|\Delta m| = 1,3,\ldots$) are induced as well. In addition, at $\theta = 54.7°$ the secular dipolar interaction is removed. In this tilted frame the level-matching lines are expected to be broadened by the underlying tunneling linewidths.

At low temperatures the methyl groups have their ground-state manifold dominated by rotational tunneling. In most cases, the tunneling energy splitting can be successfully modeled by a single-particle Hamiltonian with an effective potential of threefold symmetry.[4] Due to the coherent tunneling the threefold-degenerate torsional ground state is split into an A state of spin $\frac{3}{2}$ and a degenerate pair of E symmetry states of spin $\frac{1}{2}$ (E^a and E^b). The tunneling splitting ω_T, which depends on the potential barrier hindering the reorientation of the group, is the energy difference between the E and A states, Fig. 1.

When torsional coupling between methyl groups becomes non-negligible, the ground torsional states split further. Weak[5] and strong[6] torsional interactions were investigated to explain the observation in dimethyl sulfide. A straightforward explanation of the spectra was obtained when pairs of noninteracting CH_3 groups were introduced.[1] In such a situation the torsional energies for group I and group II satisfy $[\mathcal{H}_T(\mathrm{I}) + \mathcal{H}_T(\mathrm{II})]\Psi_\mathrm{I}\Psi_\mathrm{II} = (E_\mathrm{I} + E_\mathrm{II})\Psi_\mathrm{I}\Psi_\mathrm{II}$. The 2^6 nuclear spin functions of a methyl pair are reduced under the direct product group according to $16|AA\rangle + 8(|AE^a\rangle + |AE^b\rangle + |E^aA\rangle + |E^bA\rangle) + 4(|E^aE^a\rangle + |E^aE^b\rangle + |E^bE^a\rangle + |E^bE^b\rangle)$. The maximum spin of the product states is 3 for $|AA\rangle$, 2 for $|AE\rangle$, and 1 for $|EE\rangle$. The energy differences between the

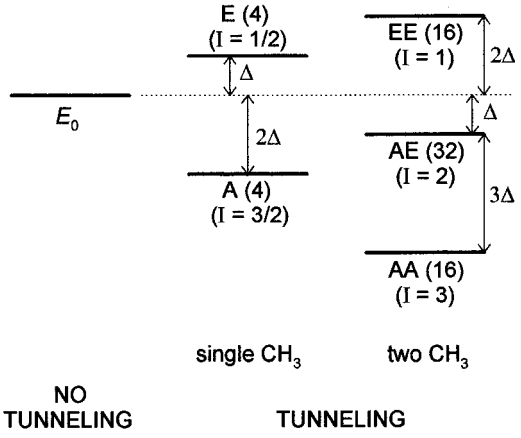

FIG. 1. The torsional ground-state manifolds of a single rotator CH_3 and of two noninteracting CH_3 rotators. Due to tunneling, the A-symmetry state of a single rotator is shifted downward by 2Δ from E_0 and the E symmetry state (E^a,E^b) upward by Δ. The splitting 3Δ is defined as the tunneling splitting $\hbar\omega_T$. The numbers in brackets next to the symmetry symbol denote the degeneracy of the torsional states. The energy of two CH_3 states is the sum of energies of a single CH_3 state. If the magnetic field is switched on the Zeeman states split. The multiplicity is $2I+1$, see Fig. 5.

AA and AE states and the AE and EE states are both equal to $\hbar\omega_T$, Fig. 1.

In this work spectra of strongly hindered methyl groups in four different lattices are shown, which demonstrate that the CH_3 groups do not interact. The matrix elements of the dipolar Hamiltonian are employed to second order. With the dependence of the spectra on the tilt angle the nature of the population transfer transitions is easily identified. It was shown[7] that, assuming that the populations of the matched levels equalize and that spin diffusion among methyl groups is negligible, the calculated magnetization changes for isolated CH_3 groups are in good agreement with the experiment. The calculated magnetization changes in level matchings involving two noninteracting CH_3 groups reproduce the observation well. However, the origin of the larger linewidth of level-matching peaks which involve the EE states—this most likely indicates a weak torsion-torsion coupling—remains unexplained.

II. TRANSITION PROBABILITY

For two noninteracting equivalent CH_3 groups in a magnetic field, the energies of the ground torsional states $|\xi m\rangle$ with symmetry ξ and magnetic quantum number m are $E_{\xi m}=-\hbar(n\omega_T+m\omega_Z)$, where $\hbar$ is Planck's constant, and n takes on values -1, 0, and 1 for the $|AA\rangle$, $|AE\rangle$, and $|EE\rangle$ states, respectively. The symmetry-adapted eigenstates $|\xi m\rangle$ are products of torsional and Zeeman vectors. They are usually written as $|(\xi_I\xi_{II})^T(\xi_I\xi_{II})^Z m\rangle$, where ξ_k denotes the symmetry of group k. Here T and Z denote torsional states and Zeeman states, which are the complex conjugate of each other.

The dipolar Hamiltonian $\mathcal{H}_D$ is a sum of intragroup and intergroup operators, $\mathcal{H}_D^{\rm intra}+\mathcal{H}_D^{\rm inter}$. The symmetry-adapted form[8] of the intragroup dipolar Hamiltonian is

$$\mathcal{H}_D^{\rm intra}=\hbar\omega_D^{\rm intra}\sum_{\mu=-2}^{+2}(-1)^\mu[U_A^{-\mu}V_A^\mu+U_{E^a}^{-\mu}V_{E^b}^\mu+U_{E^b}^{-\mu}V_{E^a}^\mu], \tag{1}$$

where $\hbar\omega_D^{\rm intra}$ is the proton dipolar energy within a CH_3 group and the spatial U_ξ and the spin V_ξ operators are defined for the point group C_3. To symmetrize the intergroup dipolar Hamiltonian, the symmetries of the two methyl groups have to be taken into account. It may be written as

$$\mathcal{H}_D^{\rm inter}=\hbar\omega_D^{\rm inter}\sum_{\mu=-2}^{2}(-1)^\mu\sum_{\xi_I\xi_{II}}U_{\xi_I\xi_{II}}^{-\mu}V_{\tilde{\xi}_I\tilde{\xi}_{II}}^{\mu}, \tag{2}$$

where $\hbar\omega_D^{\rm inter}$ is the intergroup proton dipolar energy and $\tilde{\xi}_k$ denotes the complex conjugate of ξ_k. The operators $U_{\xi_I\xi_{II}}$ and $V_{\xi_I\xi_{II}}$ are written[9,10] in the standard form

$$X_{\xi_I\xi_{II}}=\sum_{i=1}^{3}\sum_{j=4}^{6}S_{\xi_I i}S_{\xi_{II}j}X_{ij}, \tag{3}$$

where the transformation matrix S is defined for a CH_3 group and the subscripts i and j label the protons of group I and group II, respectively. In evaluating the matrix elements of $\mathcal{H}_D$, the spin- and space-dependent matrix elements may be calculated separately, since the spatial and spin degrees of freedom are separable. Symmetry arguments may be employed to identify which matrix elements do not vanish. The symmetry of $\mathcal{H}_D$ which drives transitions between two spin-torsional states is selected by the symmetry multiplication rules: $E^{a,b}A=E^{a,b}$ and $E^aE^b=A$.

The $|\Delta m|=1$ and $|\Delta m|=2$ level-matching transitions are first order. The transition rate between the initial $|\xi_i^T\xi_i^Z m_i\rangle$ and final state $|\xi_f^T\xi_f^Z m_f\rangle$ is proportional to $|\langle\xi_f^T\xi_f^Z m_f|\mathcal{H}_D^{\xi_D^T}\mathcal{H}_D^{\xi_D^Z}|\xi_i^T\xi_i^Z m_i\rangle|^2$. The selection rules for the symmetry and the magnetic quantum number are $\xi_f^T=\xi_D^T\times\xi_i^T$, $\xi_f^Z=\xi_D^Z\times\xi_i^Z$, and $|m_f-m_i|=0,1,2$. In first order, $\mathcal{H}_D^{\rm intra}$ and $\mathcal{H}_D^{\rm inter}$ induce, respectively, single-group and two-group symmetry-conversion transitions. For example, consider the transition between the single-group states $|AA-\frac{3}{2}\rangle$ and $|E^aE^b+\frac{1}{2}\rangle$ due to the terms with $\mu=2$ in Eq. (1). These contain spin operators like $I_i^+I_j^+$ and connect states whose magnetic quantum numbers differ by 2. Symmetry multiplication rules show that matrix elements such as

$$\left\langle E^aE^b+\frac{1}{2}\left|(U_{12}^{-2}+\varepsilon U_{23}^{-2}+\varepsilon^*U_{31}^{-2})(I_1^+I_2^++\varepsilon^*I_2^+I_3^++\varepsilon I_3^+I_1^+)\right|AA-\frac{3}{2}\right\rangle \tag{4}$$

are nonzero. Consequently, when the states $|AA-\frac{3}{2}\rangle$ and $|E^aE^b+\frac{1}{2}\rangle$ become degenerate at a level-matching resonance the matrix element (4) determines the transition probability which drives the population equilibration.

We may also investigate the dipolar terms with $\mu=1$ and consider transitions between two-group states $|(E^aE^a)^T(E^bE^b)^Z-1\rangle$ and $|(AA)^T(AA)^Z-2\rangle$. These states are coupled by the spin operators $I_i^0I_j^+$. One of the contributing matrix elements is

$$\langle(E^aE^a)^T(E^bE^b)^Z-1|U_{E^bE^b}^{-1}V_{E^aE^a}^{+1}|(AA)^T(AA)^Z-2\rangle, \tag{5}$$

where the torsional and spin operators are, see Eq. (3),

$$U_{E^bE^b}^{-1}=U_{13}^{-1}+\varepsilon U_{14}^{-1}+\varepsilon^*U_{15}^{-1}+\varepsilon U_{24}^{-1}+\varepsilon^*U_{25}^{-1}+U_{26}^{-1}+\varepsilon^*U_{34}^{-1}+U_{35}^{-1}+\varepsilon U_{36}^{-1}, \tag{6a}$$

$$V_{E^aE^a}^{+1}=V_{13}^{+1}+\varepsilon^*V_{14}^{+1}+\varepsilon V_{15}^{+1}+\varepsilon^*V_{24}^{+1}+\varepsilon V_{25}^{+1}+V_{26}^{+1}+\varepsilon V_{34}^{+1}+v_{35}^{+1}+\varepsilon^*V_{36}^{+1}. \tag{6b}$$

In this transition the spin and spatial wave functions of group I and also those of group II are converted from A to E symmetry. Since two groups are involved in the transition it must be driven by $\mathcal{H}_D^{\rm inter}$. The transition rate is therefore weaker

than the single group transitions by $(\omega_D^{\text{inter}}/\omega_D^{\text{intra}})^2$. This ratio depends on lattice geometry and could be as small as 10^{-2}.

For the $|\Delta m|=3$ and $|\Delta m|=4$ transitions which are forbidden in first-order, second-order perturbation theory has to be employed. Consider a $|\Delta m|=3$ transition from $|\alpha\rangle \equiv|(AA)^T(AA)^Z-2\rangle$ to $|\beta\rangle\equiv|(E^aE^a)^T(E^bE^b)^Z+1\rangle$. To first order the $|\alpha\rangle$ state may be written as

$$|\alpha\rangle^0+\sum_{\diamond\diamond\diamond}\frac{\langle(\xi_{\rm I}\xi_{\rm II})^T(\xi_{\rm I}\xi_{\rm II})^Zm|\mathcal{H}_D^{\text{inter}}|\alpha\rangle}{E_\alpha-E_{(\xi_{\rm I}\xi_{\rm II})^T(\xi_{\rm I}\xi_{\rm II})^Zm}}\times|(\xi_{\rm I}\xi_{\rm II})^T(\xi_{\rm I}\xi_{\rm II})^Zm\rangle^0, \tag{7}$$

where the superscript 0 indicates the zero-order state and the symbol $\diamond\diamond\diamond$ denotes the constraints; i.e., $\xi_{\rm I}^T\neq A$, $\xi_{\rm II}^T\neq A$, $\xi_{\rm I}^Z\neq A$, $\xi_{\rm II}^Z\neq A$, and $m\neq -2$. The off-diagonal terms of $\mathcal{H}_D^{\text{inter}}$ add the $|(\xi_{\rm I}\xi_{\rm II})^T(\xi_{\rm I}\xi_{\rm II})^Zm\rangle$ states to $|\alpha\rangle$. The transition from $|\alpha\rangle$ to $|\beta\rangle$ is now possible. The admixture of, for example, $|(AA)^T(AA)^Z0\rangle$ to $|\alpha\rangle$ enables $\mathcal{H}_D^{\text{inter}}$ to induce the $|\alpha\rangle$ to $|\beta\rangle$ transition. Since the admixture is approximately proportional to $\omega_D^{\text{inter}}/\omega_Z$, second-order transitions are weaker than first-order transitions by $\sim(\omega_D^{\text{inter}}/\omega_Z)^2$, which is typically $\leqslant 10^{-2}$. Therefore, to induce measurable level-matching transitions, the duration of the level matching has to be longer by $\geqslant 10^2$. Since the $|\alpha\rangle$ to $|\beta\rangle$ transitions are induced by $\mathcal{H}_D^{\text{inter}}$ at $\omega_Z=\frac{2}{3}\omega_T$, the transition rate is smaller than the first-order single-group transition by $(\omega_D^{\text{inter}}/\frac{2}{3}\omega_T)^2(\omega_D^{\text{inter}}/\omega_D^{\text{intra}})^2$. It can be shown that the third-order $|\Delta m|=5$ transition rate is smaller by $(\omega_D^{\text{inter}}/\frac{1}{5}\omega_T)^4(\omega_D^{\text{inter}}/\omega_D^{\text{intra}})^2$, which is expected at $\omega_Z=\frac{1}{5}\omega_T$.

III. EXPERIMENT

The ABC rf pulse sequence for the level matching in the rotating frame is $A_{0^\circ}(\theta)-B_{90^\circ}(\tau)-(\pi/2\text{ pulse comb})_{0^\circ}-C_{90^\circ}\tau$, shown Fig. 2(a). The subscripts 0° and 90° refer to the phase of the pulse. The pulse $A(\theta)$ on exact resonance rotates the high-field equilibrium magnetization M_0 by θ degrees off the z axis. After the pulse A is turned off, the frequency of the transmitter is switched from the Larmor frequency ω_0 to a predetermined off-resonance value ω in a few μs, so that the slightly off-resonance pulse B (which is phase shifted by $+90°$ with respect to the pulse A) generates an effective field H_e along which the rotated magnetization is spin locked. After the pulse B is turned off, the frequency is switched back to ω_0. The comb of $\pi/2$ pulses which follows is on resonance and the delay between the $\pi/2$ pulses is set at $\sim 10T_2$. The frequency is switched back to the off-resonance value ω before the pulse C is turned on. The pulse C generates the same effective field H_e as the pulse B. Finally, the frequency is switched again to the resonant value ω_0 to allow on-resonance detection of the signal following the pulse C.

A comb of $\pi/2$ pulses, applied before the pulse C, saturates the Zeeman states. The magnetizations during the ABC sequence without the comb, AB-t-C, are shown in Fig. 2(b). M_B represents the magnetization along the tilted effective field $\mathbf{H}_e$ at the end of the pulse B. During the delay

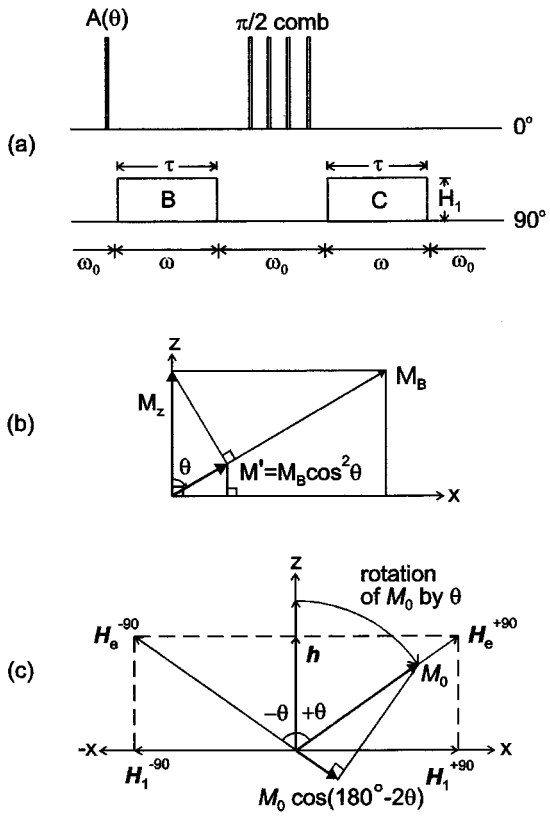

FIG. 2. (a) The rf pulse sequence used for Zeeman-tunneling level matching in the rotating frame. The 0° and 90° refer to the phases. The θ-degree pulse A and the $\pi/2$-pulse comb are on resonance frequency ω_0, while the pulses B and C of duration τ and of magnitude H_1 are off resonance. The time delay between the $\pi/2$ pulses of the comb was set at 300 μs. (b) The magnetizations arising when the comb is not applied in the tilted frame experiment. M_B represents the magnetization at the end of the pulse B. Because of the long T_1, the projection of M_B onto the z axis, M_z, remains essentially unchanged during the delay time between B and C. In such a situation, this M_z results in a magnetization M' already at the beginning of the pulse C. (c) After the pulse $A(\theta)$ rotates the magnetization M_0 it becomes spin locked along the effective field $\mathbf{H}_e^{+90^\circ}$ (which is a vector sum of $\mathbf{H}_1^{+90^\circ}$ and the off field $h\hat{\mathbf{z}}$). However, if the field $\mathbf{H}_1$ is applied along the negative x axis only a smaller Zeeman polarization $M_0\cos(180^\circ-2\theta)$ is projected along the corresponding effective field $\mathbf{H}_e^{-90^\circ}$ at the beginning of the pulse B.

$t(\gg T_2)$, the x component of M_B is phased out while its z component M_z remains unchanged, since the spin-lattice relaxation time is very long. After the pulse C is switched on, the magnetization component perpendicular to $\mathbf{H}_e$ decays to zero due to the spin-spin relaxation in the rotating frame. The magnetization, $M'=M_B\cos^2\theta$, which is the projection of M_z onto the effective field $\mathbf{H}_e$, characterizes a Zeeman polarization at the beginning of the pulse C. At $\theta=54.7°$, for example, M' is equal to $\sim 0.33M_B$, which is very large (unless M_B is small compared to M_0). In this case the tunneling to Zeeman polarization transfer during the pulse C is not as efficient as expected even when a level matching is perfectly fulfilled. Therefore, removing M_z by applying the comb is essential for any tilted-frame level-matching experiments.

The Larmor condition was established by setting the pa-

rameters which result in a null signal following a single rf pulse. If the effective field H_e, which is large compared to the local field in the rotating frame H_L', is maintained much longer than the spin-spin relaxation time in the rotating frame T_2', the magnetization becomes parallel to H_e and the magnitude is proportional to the off-field $h=(\omega_0-\omega)/\gamma$, where γ is the proton gyromagnetic ratio. This off-field dependence of the magnetization provides a reliable method of determining the resonance condition precisely.

Maximizing the signal following a spin-locking pulse sequence is not sufficient for the phase setup of the pulses B and C in a tilted-frame experiment, in which the pulse A rotates the magnetization by $+\theta$ degrees as shown in Fig. 2(c). To obtain an effective field $\mathbf{H}_e^{+90^\circ}$ parallel to the rotated magnetization, $\mathbf{H}_1$ should be along the positive x axis with $\mathbf{h}$ in the positive z direction. This is indicated as $\mathbf{H}_1^{+90^\circ}$. If $\mathbf{H}_1$ is in the negative x direction, however, the magnetization along the resulting effective field $\mathbf{H}_e^{-90^\circ}$ will be $M_0\cos(180^\circ-2\theta)$, which is much smaller than M_0. Therefore it has to be determined whether $\mathbf{H}_1$ is in the positive x direction or in the negative x direction. The signal following an rf pulse with strength $H_1 \gg H_L'$ and duration $\tau \gg T_2'$, was used to determine the phase. First, the phase of the pulse is set between 0° and 180° by adjusting it to give a positive signal when $\omega_0 > \omega$ and a negative one when $\omega_0 < \omega$. Next the signal following the spin-locking pulse sequence is maximized to have the H_1 along the positive x direction.

IV. PROTON MAGNETIZATION CHANGES DUE TO POPULATION EQUILIBRATION OF MATCHED ZEEMAN-TUNNELING ENERGY LEVELS

Consider a pair of noninteracting equivalent CH_3 groups in a magnetic field H_0, in equilibrium with the lattice. The populations of spin-torsional states $|\xi m\rangle$, in the high-temperature approximation, should meet the following constraints: (i) the total population of the states is unity, (ii) the ratio of two adjacent Zeeman level populations is $1-\delta_0$, and (iii) the ratio of two adjacent tunneling level populations is $1-\delta_T$, where $\delta_0=\hbar\omega_0/k_BT_L$, $\delta_T=\hbar\omega_T/k_BT_L$, and $\omega_0=\gamma H_0$. Here T_L and k_B are the lattice temperature and the Boltzmann constant, respectively. The population of the $p_{|\xi m\rangle}$ state that satisfies the constraints is $\frac{1}{64}(1+m\delta_0+n\delta_T)$. As ω_T is small compared to ω_0, the third term $n\delta_T$ is negligible. The population is then

$$p_{|\xi m\rangle}=\tfrac{1}{64}\ (1+m\delta_0). \tag{8}$$

The magnetization is calculated from

$$M=\gamma\hbar\sum_{\xi m} D_{|\xi m\rangle}p_{|\xi m\rangle}m, \tag{9}$$

where $D_{|\xi m\rangle}$ is the degeneracy of the $|\xi m\rangle$ state. Equations (8) and (9) give the initial equilibrium magnetization $M_0=\frac{3}{2}\gamma\hbar\delta_0$. Since the magnetization is conserved during spin locking the Zeeman temperature T_Z is lowered by $\sim\omega_Z/\omega_0$, while the tunneling system remains in equilibrium with the lattice. The Zeeman splitting ω_Z in the rotating frame is of the same magnitude as ω_T. Therefore, immediately after the spin locking the Zeeman polarization is larger by $\sim\omega_0/\omega_Z$ than the tunneling polarization. In such a situation, when two or more spin-torsional states with different populations are matched experimentally their populations become equal after a sufficiently long time is allowed for mixing, thereby resulting in a magnetization change.

The ground torsional state manifold of two methyl groups in a progressively larger magnetic field is shown in Fig. 5. Seven level-matching resonances are predicted at $\omega_Z=n\omega_T$, with $n=\frac{1}{5}$, $\frac{1}{4}$, $\frac{1}{3}$, $\frac{1}{2}$, $\frac{2}{3}$, 1, and 2. When the Zeeman splitting during the pulse B satisfies, for example, the $\omega_Z=\frac{2}{3}\omega_T$ resonance, two level matchings occur: one between $|EE0\rangle$ and $|AA-3\rangle$ (LM1) and another between $|EE+1\rangle$ and $|AA-2\rangle$ (LM2). When the full equilibration of their populations is achieved the populations are

$$p_{\mathrm{LM1}}(\mathrm{eq})=\tfrac{1}{9}\ [8p_{|EE0\rangle}+p_{|AA-3\rangle}]=\tfrac{1}{64}\ (1-\tfrac{1}{3}\delta), \tag{10a}$$

$$p_{\mathrm{LM2}}(\mathrm{eq})=\tfrac{1}{6}\ [4p_{|EE+1\rangle}+2p_{|AA-2\rangle}]=\tfrac{1}{64}\,, \tag{10b}$$

with $\delta=\hbar\omega_Z/k_BT_Z$. It is assumed that the population transfer is an exponential function of mixing time τ with a characteristic Zeeman-tunneling coupling time constant $T_{\mathrm{ZT}\rho}$,[7,11]

$$p_{|\xi m\rangle}(\tau)=p_{|\xi m\rangle}(0)+[p_{|\xi m\rangle}(\mathrm{eq})-p_{|\xi m\rangle}(0)]\times[1-\exp(-\tau/T_{\mathrm{ZT}\rho})], \tag{11}$$

where $p_{|\xi,m\rangle}(0)$ is the initial population, Eq. (8), and $p_{|\xi,m\rangle}(\mathrm{eq})$ is the equilibrium populations, respectively. Equation (11) gives the populations of the matched states as a function of mixing time,

$$p_{|EE0\rangle}(\tau_B)=\tfrac{1}{64}\ [1-\tfrac{1}{3}\ \delta(1-\Omega)], \tag{12a}$$

$$p_{|EE+1\rangle}(\tau_B)=\tfrac{1}{64}\ (1+\delta\Omega), \tag{12b}$$

$$p_{|AA-3\rangle}(\tau_B)=\tfrac{1}{64}\ [1-\tfrac{1}{3}\ \delta(1+8\Omega)], \tag{12c}$$

$$p_{|AA-2\rangle}(\tau_B)=\tfrac{1}{64}\ (1-2\delta\Omega), \tag{12d}$$

where $\Omega=\exp(-\tau_B/T_{\mathrm{ZT}\rho})$ and τ_B is the duration of the pulse B. The states which are not matched retain their initial populations given by Eq. (8). Due to the population equilibration at the $\omega_Z=\frac{2}{3}\omega_T$ resonance, the magnetization reduces from M_0 to

$$M_B(\tau_B)=\tfrac{1}{24}\ (19+5\Omega)M_0\,. \tag{13}$$

The population has been transferred from the highly populated $|EE0\rangle$ and $|EE+1\rangle$ states, respectively, to the $|AA-3\rangle$ and $|AA-2\rangle$ states. This implies that a fraction of methyl pairs have undergone the EE to AA symmetry conversion. When a sufficient mixing time is allowed to complete the population equilibration, the Zeeman polarization of $\frac{5}{24}M_0$ will be transferred to the tunneling states.

Before the pulse C is turned on, the Zeeman system is prepared at an infinite temperature so that when the same level-matching resonance is reestablished during the pulse C, the polarization transfer runs in the reverse direction. The

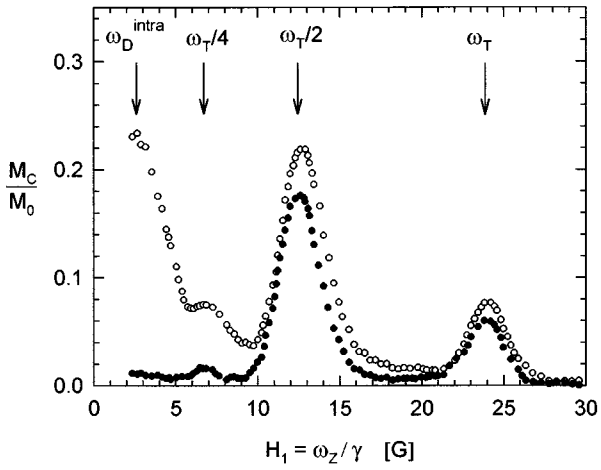

FIG. 3. Spectra at 30 K of dimethyl sulfide obtained without (empty circles) and with (filled circles) a comb of $\pi/2$ pulses. The observed peaks are labeled by arrows with the underlying matching resonance. The mixing time τ and the tilt angle θ were 1 ms and 90°, respectively. At the first stage of the polarization transfer (pulse B) there is some loss of order to the dipolar reservoir which is then destroyed by the $\pi/2$ pulse comb. During the reverse transfer (pulse C) some order is again lost to the dipolar reservoir. These losses are negligible at large magnetic field, i.e., at $\omega_Z \gg \omega_D$.

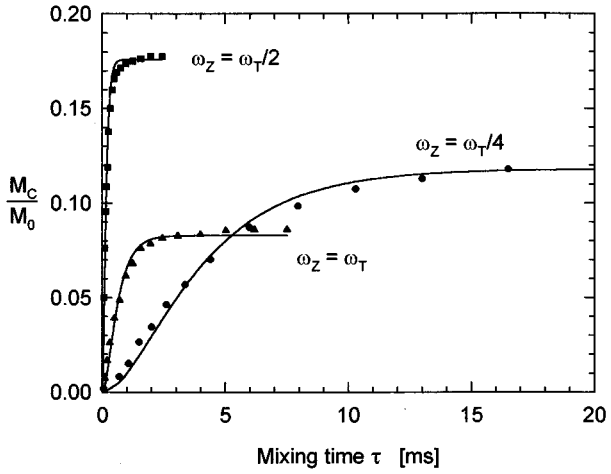

FIG. 4. Plot of the magnetization M_C in dimethyl sulfide at 30 K as a function of mixing time τ in the rotating frame with $\theta = 90°$. Each growth pattern of M_C (at a particular H_1) is labeled with the matching resonance at which the Zeeman to tunneling (pulse B) and the following tunneling to Zeeman (pulse C) polarization transfers have been measured. In pulse B of duration τ the transfer is proportional to $[1-\exp(-\tau/T_{ZT\rho})]$ and the same applies in pulse C of duration τ. For this reason the data were fitted to $K[1-\exp(-\tau/T_{ZT\rho})]^2$ with adjustable parameters K and $T_{ZT\rho}$, see Table I.

saturation of spins is equivalent to averaging the populations within a symmetry. The populations at the beginning of the pulse C are then

$$p_{|EEm\rangle}(\tau_C=0) = \tfrac{1}{64}\,[1-\tfrac{5}{12}\,\delta(1-\Omega)], \tag{14a}$$

$$p_{|AEm\rangle}(\tau_C=0) = \frac{1}{64}, \tag{14b}$$

$$p_{|AAm\rangle}(\tau_C=0) = \tfrac{1}{64}\,[1+\tfrac{5}{12}\,\delta(1-\Omega)]. \tag{14c}$$

The population of the AA states is now larger than the EE state population. This is as expected, since the tunneling states became polarized during the pulse B. The three populations in Eq. (14) show a Boltzmann distribution in the high-temperature approximation. Such a distribution of the tunneling population also appears in the $\omega_Z = 2\omega_T$ resonance. This Boltzmann distribution is maintained during the pulse C if level matchings occur only between the AA and EE states. The populations of the AA and EE states then decrease and increase, respectively, by the same magnitude, while the AE states maintain the populations at $\tau_C = 0$. In other resonances, e.g., $n = \frac{1}{4}, \frac{1}{3}, \frac{1}{2}$, and 1 the tunneling populations at $\tau_C = 0$ are not described by the Boltzmann statistics. Since no spin diffusion is allowed for in the calculation, the occurrence of the Boltzmann distribution of the tunneling populations during the pulse C in the $\omega_Z = \frac{2}{3}\omega_T$ and $\omega_Z = 2\omega_T$ resonances is solely due to the double-symmetry conversion between the AA and EE states.

When the level matchings LM1 and LM2 are reintroduced during the pulse C with duration τ equal to τ_B, the magnetization growth along the effective field will be

$$M_C(\tau) = \tfrac{25}{432}\,[1-\exp(-\tau/T_{ZT\rho})]^2 M_0. \tag{15}$$

If the pulses B and C are both longer than $5T_{ZT\rho}$, M_C is calculated to be 5.8% of M_0. The magnetization detected in the experiment is the projection of M_C onto the x axis, $M_C \sin\theta$, which is for $\theta = 54.7°$ only 4.7% of M_0.

V. RESULTS AND DISCUSSION

In the low-field NMR in solids, the energy splittings due to local dipolar fields are comparable to the Zeeman splitting. The polarization transfer between Zeeman and dipolar systems therefore has to be considered in level matching in

TABLE I. Listed are the Zeeman-tunneling coupling times $T_{ZT\rho}$ obtained from fitting the function $[1-\exp(-\tau/T_{ZT\rho})]^2$ to the magnetizations M_C, in dimethyl sulfide, which evolves as a function of the mixing time τ in the rotating frames with $\theta = 90°$ and with $\theta = 54.7°$. Note that the value of $T_{ZT\rho}$ at $\omega_Z = 2\omega_T$ is for the CH_3 in methylmalonic acid. The quoted accuracy is the standard deviation.

ω_Z	θ	$T_{ZT\rho}$ (ms)
$\frac{1}{4}\,\omega_T$	90°	2.8 ±0.1
	54.7°	6.2 ±0.4
$\frac{1}{3}\,\omega_T$	90°	Not observed
	54.7°	1.6 ±0.1
$\frac{1}{2}\,\omega_T$	90°	0.10±0.01
	54.7°	0.21±0.01
$\frac{2}{3}\,\omega_T$	90°	Not observed
	54.7°	1.9 ±0.02
ω_T	90°	0.45±0.02
	54.7°	0.31±0.03
$2\omega_T$	90°	Not observed
	54.7°	3.13±0.2

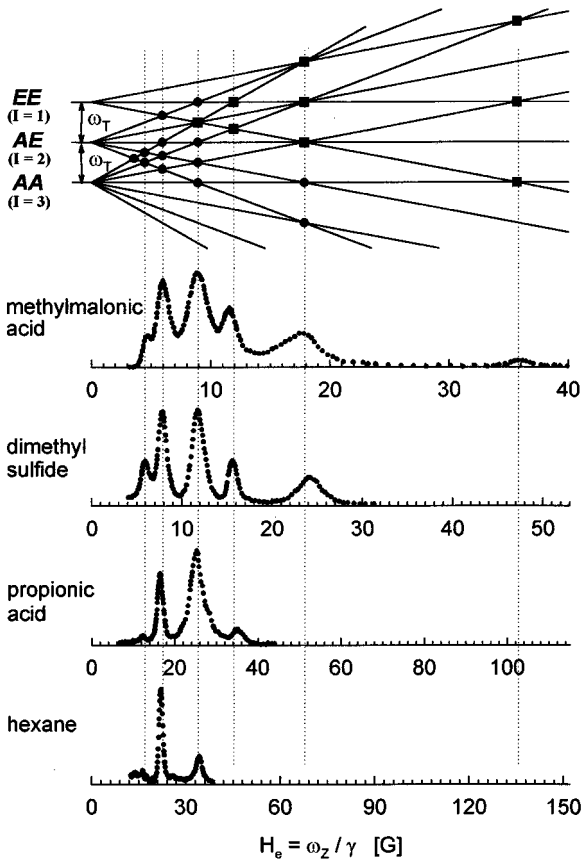

FIG. 5. At the top is the energy level diagram of two noninteracting equivalent CH_3 groups with the matching resonances at $\omega_Z = n\omega_T$ for $n = \frac{1}{5}, \frac{1}{4}, \frac{1}{3}, \frac{1}{2}, \frac{2}{3}$, 1, and 2 shown. Vertical dotted lines are drawn at the observed resonances, $n = \frac{1}{4}, \frac{1}{3}, \frac{1}{2}, \frac{2}{3}$, 1, and 2. Squares indicate the level matchings at which the AA-EE transitions occur. Spectra at 30 K of methylmalonic acid, dimethyl sulfide, propionic acid, and hexane in the tilted rotating frame with $\theta = 54.7°$ are shown. The mixing times τ were all 10 ms. Note that the H_e axes for all the spectra are adapted so that all ω_T coincide.

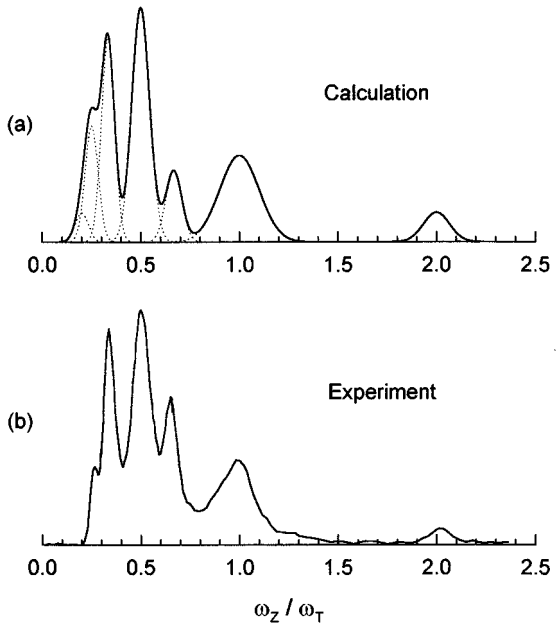

FIG. 6. (a) A model spectrum for a pair of noninteracting equivalent methyl groups. Equal populations of matched energy levels were assumed. The areas under the peaks were adjusted to represent the calculated intensities. The line shapes were modeled to be Gaussian with widths selected to match the observed spectrum. (b) The experimental spectrum of methylmalonic acid ($HOOCCHCH_3COOH$). Both in (a) and (b), the area under the each peak is normalized with respect to the entire area.

the rotating frame. Since the dipolar energy levels are polarized during the pulse B, the signal following the pulse C (at low H_e) is due to the polarization transfer from the dipolar system as well as from the tunneling system. To make the small tunneling peaks observable the dipolar polarization has to be erased by applying a $\pi/2$-pulse comb before the pulse C. The effect of the $\pi/2$ comb on the level-matching spectrum is shown in Fig. 3. Without the comb, the dipolar signal is of nearly the same amplitude as the strongest tunneling peak at $\omega_Z = \frac{1}{2}\omega_T$.

In all the studied materials, the measurement with a mixing time τ of ~ 0.1 ms reveals level-matching resonances at $\omega_Z = \frac{1}{2}\omega_T$ and at $\omega_Z = \omega_T$, Fig. 3. These transitions are driven by the intragroup dipolar interaction in first order. This observation manifests the single-particle picture for the rotational tunneling of methyl groups. Since the magnetization changes are the direct results of the population equilibration, the magnetizations following the pulses B and C depend on τ strongly. When the mixing time τ is increased further so that the weaker transitions bring about a measurable polarization transfer as well, a second-order peak at $\omega_Z = \frac{1}{4}\omega_T$ becomes observable. Generally second-order transitions become measurable if mixing times beyond 5 ms are employed.

The growth of the magnetization M_C in dimethyl sulfide is presented as a function of mixing time τ, in Fig. 4. It was shown in Sec. IV that M_C is proportional to $[1 - \exp(-\tau/T_{ZT\rho})]^2$, which allows determination of the Zeeman-tunneling polarization transfer rate, $T_{ZT\rho}^{-1}$. For dimethyl sulfide the $T_{ZT\rho}$ values obtained from the magnetization growth patterns are listed in Table I.

The second-order level-matching transitions, for example, at the $\omega_Z = \frac{1}{4}\omega_T$ resonance are weaker by $(\omega_D^{\text{inter}}/\frac{1}{4}\omega_T)^2(\omega_D^{\text{inter}}/\omega_D^{\text{intra}})^2$, than the first-order transitions at the $\omega_Z = \frac{1}{2}\omega_T$ resonance driven by $\mathcal{H}_D^{\text{intra}}$. Hence, the ratio of the two rates is

$$\frac{(T_{ZT\rho}^{-1})_{(1/4)\omega_T}}{(T_{ZT\rho}^{-1})_{(1/2)\omega_T}} = 16f^4\left(\frac{\omega_D^{\text{intra}}}{\omega_T}\right)^2, \tag{16}$$

where $f = \omega_D^{\text{inter}}/\omega_D^{\text{intra}}$. The ratio $\omega_D^{\text{intra}}/\omega_T$ in dimethyl sulfide is ~ 0.10, Fig. 3. As the ratio $(T_{ZT\rho}^{-1})_{(1/4)\omega_T}/(T_{ZT\rho}^{-1})_{(1/2)\omega_T}$ is 0.035, Table I, the ratio of the intergroup to the intragroup dipolar energy, f, equals 0.68 ± 0.06. Since the dipolar energy is inversely proportional to the cube of the proton-proton distance, the average distance between two protons belonging to adjacent methyl groups turns out to be 2.0 ± 0.2 Å; the intragroup proton-proton distance was taken to be 1.78 Å. Such a small distance (2.0 Å) would be possible only when two CH_3 groups under consideration belong to adjacent CH_3SCH_3 molecules.

In the tilted rotating frame, the dipolar Hamiltonian which couples energy states with magnetic quantum numbers differing by 1 is proportional to $\sin\theta\cos\theta$, while the interaction driving the $|\Delta m|=2$ transitions is proportional to $\sin^2\theta$. The same argument can be extended to second-order transitions. The $|\Delta m|=4$ transition peak at $\omega_Z=\frac{1}{4}\omega_T$ then decreases as the effective field is tilted away from the x-y plane, while the $|\Delta m|=3$ transition lines at $\omega_Z=\frac{1}{3}\omega_T$ and $\omega_Z=\frac{2}{3}\omega_T$ increase. Level-matching spectra of methyl groups in four polycrystalline materials, recorded in the rotating frame with $\theta=54.7°$, are shown in Fig. 5, together with the energy level diagram of two equivalent noninteracting CH_3 groups. The mixing times were all 10 ms during which the level-matching peaks brought about by second-order processes grew substantially. The resonances at $\omega_Z=n\omega_T$, with $n=\frac{1}{4}$, $\frac{1}{3}$, $\frac{1}{2}$, $\frac{2}{3}$, 1, and 2 were observed, however, the $\omega_Z=\frac{1}{5}\omega_T$ resonance peak due to the $|\Delta m|=5$ transitions between the $|AE+2\rangle$ and $|AA-3\rangle$ states, has not been observed. These third-order transitions are too weak to cause a measurable polarization transfer even with the mixing time of 100 ms.

If the $|EE\rangle$ states are split by the presence of methyl-methyl coupling, the resonances involving these states could be broader than the resonances occurring between $|AA\rangle$ and $|AE\rangle$ states. When the linewidths at $\omega_Z=\frac{2}{3}\omega_T$ and $2\omega_T$ resonances are compared with other linewidths, no systematic difference is found, as expected of ''noninteracting,'' or indeed very weakly interacting methyl groups.

The calculated spectrum for the full population equilibration is shown in Fig. 6. It is in good agreement with the experimental spectrum of methylmalonic acid. The protons which do not belong to a methyl group do not contribute to the polarization transfer. Therefore the magnetization growth M_C has to be compared to the fraction of M_0 which is due to methyl protons only. In dimethyl sulfide, the published results[6,12] indicate that the two methyl groups in a molecule are in different hindering potentials, having ω_T of 100 KHz and 750 KHz. The $\omega_Z=\frac{2}{3}\omega_T$ resonance peak, detected at $H_e=15.6$ G, Fig. 5, demonstrates that two groups involved in the transitions both have $\omega_T/2\pi=100$ KHz. This observation is in accord with the small intergroup proton-proton distance (obtained from the $T_{ZT\rho}$ measurements).

In conclusion, applying a comb of $\pi/2$ pulses between the B and C pulses improves the level matching in a tilted rotating frame significantly. Tilting the effective field in the rotating frame makes it possible to identify the change of the magnetic quantum number during a level-matching transition. Most spectra of strongly hindered CH_3 groups so far are consistent with the existence of a two-equivalent-noninteracting-CH_3-group manifold. Among the observed resonances the $\omega_Z=\frac{2}{3}\omega_T$ and the $\omega_Z=2\omega_T$ resonances demonstrate that two CH_3 groups undergo symmetry conversion simultaneously. The magnetization changes calculated using the population equilibration assumption reproduce the observations well. Furthermore, the magnetization change as a function of mixing time gives the Zeeman-tunneling coupling time $T_{ZT\rho}$ from which the average intergroup proton-proton distance can be estimated.

ACKNOWLEDGMENT

Support from the National Science and Engineering Research Council, Ottawa is gratefully acknowledged.

[1] C. Choi and M. M. Pintar, Phys. Rev. Lett. **76**, 527 (1996).
[2] W. I. Goldberg and M. Lee, Phys. Rev. **140**, A1261 (1965).
[3] J. R. Franz and C. P. Slichter, Phys. Rev. **148**, 287 (1966).
[4] W. Press, *Single-Particle Rotations in Molecular Crystals*, Vol. 92 of Springer Tracts in Modern Physics (Springer, New York, 1981).
[5] D. Smith, Chem. Phys. Lett. **188**, 349 (1992).
[6] P. J. McDonald and M. Pinter-Krainer, Mol. Phys. **84**, 1021 (1995).
[7] K. R. Sridharan, W. T. Sobol, and M. M. Pintar, J. Chem. Phys. **82**, 4886 (1985).
[8] F. Apaydin and S. Clough, J. Phys. C **1**, 932 (1968).
[9] A. H. Vuorimäki and M. Punkkinen, J. Phys. Condens. Matter **2**, 993 (1990).
[10] J. Peternelj, A. Z. Damyanovich, and M. M. Pintar, Phys. Rev. B **49**, 3322 (1994).
[11] B. S. Bharaj and M. M. Pintar, Phys. Rev. Lett. **52**, 1986 (1984).
[12] S. Clough, A. J. Horsewill, P. J. McDonald, and F. O. Zelaya, Phys. Rev. Lett. **55**, 1794 (1985).